

# OPTIMIZATION OF A SINGLE-CELL ACCELERATING STRUCTURE FOR RF BREAKDOWN TEST WITH SHORT RF PULSES

M.M. Peng<sup>\*1</sup>, M.E. Conde, G. Ha, C. Jing<sup>2</sup>, W. Liu, J.G. Power, J. Seok, J.H. Shao<sup>†</sup>,  
E.E. Wisniewski, Argonne National Laboratory, Lemont, IL, USA  
J. Shi, Tsinghua University, Beijing, People's Republic of China  
<sup>1</sup>also at Tsinghua University, Beijing, People's Republic of China  
<sup>2</sup>also at Euclid Techlabs, Bolingbrook, IL, USA

## Abstract

RF breakdown is one of the major limitations to achieve high gradient acceleration for future structure-based normal conducting linear colliders. Previous statistic research shows that the breakdown rate is proportional to  $E_a^{30} \times t_p^5$ , which indicates that the accelerating gradient ( $E_a$ ) could be improved by using shorter RF pulses ( $t_p$ ). An X-band 11.7 GHz metallic single-cell structure has been designed for RF breakdown study up to 273 MV/m using short pulses ( $\sim 3$  ns) generated by a 400 MW power extractor at Argonne Wakefield Accelerator (AWA) facility. The structure has also been scaled to 11.424 GHz for the long pulse (100-1500 ns) breakdown study driven by a klystron and a pulse compressor at Tsinghua X-band High Power Test-stand (TPoT-X), with the gradient up to 246 MV/m with 200 MW input power.

## INTRODUCTION

High gradient acceleration is one of the key technologies to reduce the cost of future TeV-scale linear colliders. A major limiting factor to improve the accelerating gradient is the RF breakdown phenomenon [1, 2] which will lead to structure damage, reduced energy gain, or even beam loss. Intense experimental research has been conducted worldwide led by CERN-SLAC-KEK collaboration to study the RF breakdown dependence on accelerating structure properties, from which it has been observed that the breakdown rate (BDR) is sensitive with the accelerating gradient and the RF pulse length as  $BDR \propto E_a^{30} \times t_p^5$  [3].

Argonne Flexible Linear Collider (AFLC) [4] has therefore been proposed to significantly improve the state-of-the-art gradient by applying short RF pulses. The baseline design applies the two-beam acceleration approach in which  $\sim 20$  ns GW level RF pulses are generated from 26 GHz power extractors driven by short trains of high charge drive bunches. The corresponding accelerating gradient is above 250 MV/m in the main beam accelerators.

This research aims to study RF breakdown with a wide range of RF pulse lengths to verify the short pulse high gradient concept. It contains two parts: 1) short pulse ( $\sim 3$  ns, up to 400 MW) test driven by an X-band 11.7 GHz power extractor [5] at AWA; 2) long pulse (100-1500 ns, up to 200 MW) test driven by an X-band 11.424 GHz klystron with a pulse compressor [6] at TPoT-X [7]. A single-cell

accelerating structure has been optimized at 11.7 GHz to obtain the maximum accelerating gradient using the short RF pulses and then scaled to 11.424 GHz. In both parts, the maximum gradient is designed to be  $\sim 250$  MV/m with the available input power.

## ACCELERATING GRADIENT ANALYSIS

Figure 1 illustrates the layout of the high gradient accelerating structure for high power test, including a single high gradient accelerating cell, two matching cells, and two RF couplers.

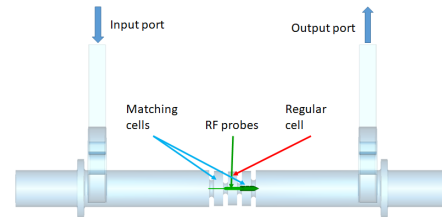


Figure 1: The simulation model of the single-cell structure for transit accelerating gradient analysis.

Detailed analysis of the structure response has been conducted in this section to determine the accelerating gradient driven by long and short RF pulses. In this section, the structure is assumed to be a  $N$ -cell traveling-wave metallic disk-loaded one with cell length of  $L$ .

### On-axis longitudinal electric field

When driven by an RF pulse with finite length (bandwidth), several  $TM_{01}$  modes with various phase advances could be excited within the bandwidth. Their space harmonics [8] also exist to satisfy the longitudinal period boundary condition at the iris.

When ignoring the structure attenuation, the on-axis longitudinal electric field can therefore be express as

$$E_z(z, t) = \sum_{k=0}^{N-1} \sum_{n=-\infty}^{\infty} E_{k,n} e^{j(\omega_k t - \beta_{k,n} z)} \quad (1)$$

where the subscript  $k, n$  denotes the  $n$ th harmonic of the  $k$ th mode,  $\omega_k$  denotes the frequency of the  $k$ th mode and its harmonics, and  $\beta$  denotes the longitudinal wave number as  $\beta_{k,n} = k\pi/NL + 2\pi n/L$ . The 0th harmonic is referred as the fundamental mode in this manuscript.

\* mpeng@anl.gov

† jshao@anl.gov

Content from this work may be used under the terms of the CC BY 3.0 licence (© 2019). Any distribution of this work must maintain attribution to the author(s), title of the work, publisher, and DOI

### Long pulse steady state analysis

When the RF pulse length is long enough so that its bandwidth is narrower than the separation between neighboring fundamental modes, only one fundamental mode (denoted as the  $m$ th mode, a.k.a. the working mode) and its space harmonics could be excited whose on-axis longitudinal electric field can be simplified from Eqn. 1 as

$$E_z(z, t) = \sum_{n=-\infty}^{\infty} E_{m,n} e^{j(\omega t - \beta_n z)} \quad (2)$$

The fundamental mode usually has the highest amplitude in forward-wave structures, which is designed for acceleration by setting its phase velocity to the speed of the beam. When considering ultrarelativistic beam, the longitudinal wave number of the fundamental mode can be derived as  $\beta_0 = \omega/c$  and the cell length is therefore set to  $L = cm\pi/\omega N$ .

The other space harmonics [8] don't contribute to the acceleration, which can be verified by the energy gain as

$$\begin{aligned} W &= \int_0^L E_z(z, t) dz = \int_0^L E_z(z, z/c) dz \\ &= \int_0^L \sum_{n=-\infty}^{\infty} E_n e^{j(\beta_0 - \beta_n)z} dz = E_0 L \end{aligned} \quad (3)$$

For the steady state, the on-axis longitudinal electric field can be simulated by the Eigen mode solver of CST Microwave Studio and the corresponding accelerating gradient can be derived as

$$E_0 = \int_0^L E_z(z) e^{j\beta_0 z} dz / L \quad (4)$$

Figure 2 shows an example of the on-axis longitudinal electric field and calculated  $E_0$  in a structure working at  $2/3\pi$  mode with three identical cells.

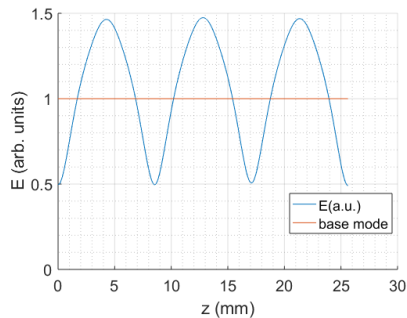


Figure 2: The amplitude distribution of the on-axis electric field and the corresponding 0th harmonic.

### Short pulse transit analysis

When the RF pulse length is short when its bandwidth is comparable or wider than the mode separation, several modes could be excited and the energy gain can be expressed as

$$\begin{aligned} W &= \int_0^L E_z(z, t) dz = \int_0^L E_z(z, z/c) dz \\ &= \sum_{k=0}^{N-1} \sum_{n=-\infty}^{\infty} \int_0^L E_{k,n} e^{j(\omega_k/c - \beta_{k,n})z} dz \end{aligned} \quad (5)$$

Since  $\int_0^L E_{k,n} e^{j(\omega_k/c - \beta_{k,n})z} dz \neq 0$  when  $k \neq m$ , the modes other than the working mode and their harmonics could also contribute to the acceleration. In this case, the accelerating gradient  $G$  is therefore defined as  $G = W/L = \int_0^L E_z(z, t) dz / L$ .

In CST Microwave Studio, time domain simulation with a series of probes along the axis needs to be conducted to obtain  $E_z(z, t)$  so as to calculate the accelerating gradient. This method is also suitable for other short pulse conditions, such as when the pulse length is shorter than the structure filling time.

Figure 3 shows the simulated results when the structure is driven by 100 ns and 3 ns RF pulses. The input pulse shapes are similar to those to be used in the high power tests. It can be observed that: 1) steady state when driven by long pulse could be reached after tens of nanosecond; 2) the ratio  $R$  defined as the peak accelerating gradient with short RF pulses to that with long pulses is only  $\sim 80\%$ , which indicates that the structure is not fully filled; 3) several fundamental modes have been excited with short pulses, which can be confirmed by the beating pattern after  $\sim 20$  ns.

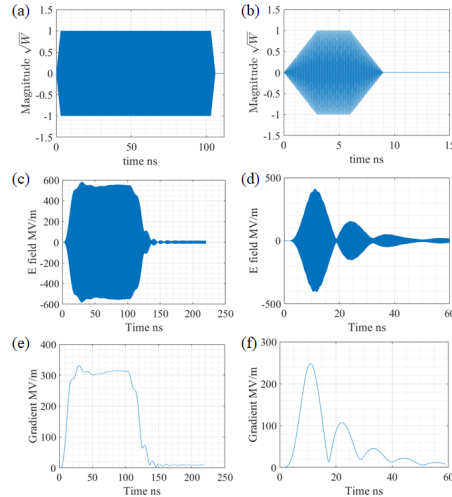


Figure 3: Comparison of the structure response driven by long pulses (left) and short pulses (right) in time domain simulation. (a-b) Input pulse shape. (c-d) Transit electric field at the center of the single cell. (e-f) Accelerating gradient evolution.

## SINGLE-CELL ACCELERATING STRUCTURE OPTIMIZATION

Based on the analysis in the previous section, a single-cell accelerating structure has been optimized to achieve the highest accelerating gradient with 3 ns short RF pulses.

The most important goal in the optimization is the accelerating gradient which is largely determined by the iris radius  $a$ . For long pulses, smaller  $a$  leads to higher shunt impedance and higher gradient at steady state. For short pulses, however, smaller  $a$  causes reduced  $R$  since the filling time is longer. Therefore,  $a$  (or the filling time) has to be optimized to compromise between the shunt impedance and  $R$ , as illustrated in Figure. 4.

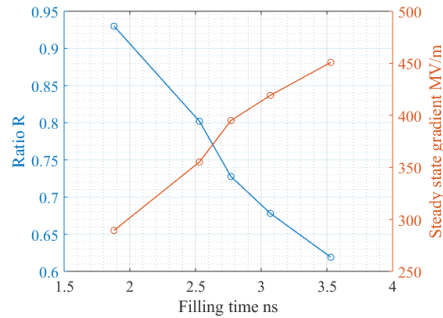


Figure 4: The stead state accelerating gradient and  $R$  as a function of the filling time.

The secondary optimization goal is the surface electric field which can be reduced by elliptical iris. The optimization of structure with round iris and elliptical iris is illustrated in Figure. 5.

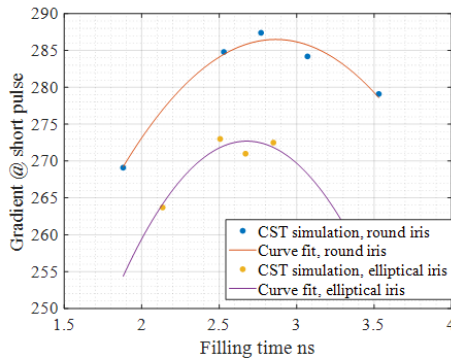


Figure 5: The accelerating gradient with short pulses as a function of filling time for both the round iris structures and the elliptical iris ones.

The detailed parameters of the optimized structure with elliptical iris are listed in Table 1.

## EXPERIMENTAL PLAN

Currently, both the 11.7 GHz and the scaled 11.424 GHz structures are under fabrication and the high power tests are planned to be conducted in the next year. A preliminary experimental setup is illustrated in Figure. 6. The diagnostics will include directional couplers to measure forward, reflected, and transmitted RF power; upstream and downstream Faraday cups to measure the dark current; and a photo-multiplier tube with a fluorescent screen to detect X-ray accompanying RF breakdown.

Table 1: Parameters of the Single Cell Structure

Parameters	Unit	Value
Resonate frequency	GHz	11.7
Iris diameter	mm	6.1
Iris thickness	mm	2.9
Elliptical major axis	mm	3.2
Elliptical minor axis	mm	1.4
Mode		$2\pi/3$
Filling time	ns	2.5
Group velocity	c	0.0114
Gradient @200 MW, long pulse	MV/m	246
Gradient @400 MW, 3 ns pulse	MV/m	273
Q		6073
r/Q	$\Omega/m$	14048
Es/Ea (steady state)		1.59

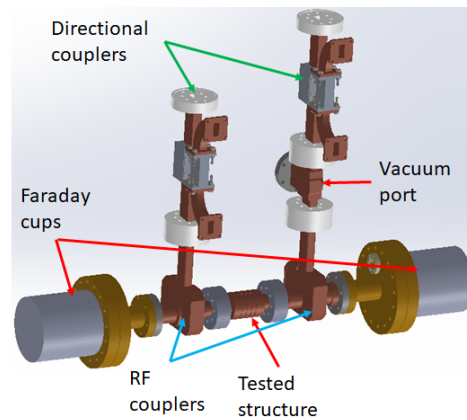


Figure 6: High power test layout.

## CONCLUSION

An X-band 11.7 GHz single-cell accelerating structure has been designed for RF breakdown test using short RF pulses ( $\sim 3$  ns). The gradient with such short pulses is defined as the average accelerating gradient along the single cell contributed by all excited  $TM_{01}$  modes. With 400 MW input power from a power extractor, the gradient is designed to reach 273 MV/m after structure optimization. The structure has also been scaled to 11.424 GHz to be tested with long RF pulses (100-1500 ns) from a klystron with a pulse compress at similar gradient for comparison. The experiments are planned in the next year.

## ACKNOWLEDGMENT

The work at AWA is funded through the U.S. Department of Energy Office of Science under Contract No. DE-AC02-06CH11357. The work by Tsinghua University is funded by the National Natural Science Foundation of China (Grant No. 11635006). We would like to thank the Tsinghua machining shop for fabricating the structures.

## REFERENCES

- [1] E. I. Simakov, V. A. Dolgashev, and S. G. Tantawi, "Advances in high gradient normal conducting accelerator structures," *Nucl. Instrum. Methods Phys. Res., Sect. A*, vol. 907, pp. 221–230, 2018.
- [2] J. Shao, *Investigations on rf breakdown phenomenon in high gradient accelerating structures*. Singapore: Springer, 2018.
- [3] A. Grudiev, S. Calatroni, and W. Wuensch, "New local field quantity describing the high gradient limit of accelerating structures," *Phys. Rev. Spec. Top. Accel. Beams*, vol. 12, no. 10, p. 102001, 2009.
- [4] C. Jing *et al.*, "Argonne flexible linear collider," in *Proc. 4th Int. Particle Accelerator Conf. (IPAC'13)*, Shanghai, China, May 2013, pp. 1322–1324.
- [5] M. Peng *et al.*, "Generation of high power short rf pulses using an x-band metallic power extractor driven by high charge multi-bunch train," in *Proc. 10th Int. Particle Accelerator Conf. (IPAC'19)*, Melbourne, Australia, May 2019, pp. 734–737. doi: 10.18429/JACoW-IPAC2019-MOPRB069.
- [6] Y. Jiang *et al.*, "The x-band pulse compressor for tsinghua thomson scattering x-ray source," in *Proc. 8th Int. Particle Accelerator Conf. (IPAC'17)*, Copenhagen, Denmark, May 2017, pp. 4214–4217. doi: 10.18429/JACoW-IPAC2017-THPIK054.
- [7] M. Peng *et al.*, "Development of Tsinghua X-Band High Power Test Facility," in *9th Int. Particle Accelerator Conf. (IPAC'18)*, Vancouver, BC, Canada, Apr. 2018, pp. 3999–4001. doi: 10.18429/JACoW-IPAC2018-THPAL150.
- [8] T. P. Wangler, *RF Linear accelerators*. John Wiley & Sons, 2008.